# GlycoFibroTyper: A Novel Method for the Glycan Analysis of IgG and the Development of a Biomarker Signature of Liver Fibrosis

Danielle A. Scott[1], Mengjun Wang[2], Stephane Grauzam[2], Sarah Pippin[1], Alyson Black[2], Peggi M. Angel[2], Richard R. Drake[2], Stephen Castellino[1], Yuko Kono[3], Don C. Rockey[4] and Anand S. Mehta[2]*

[1] Glycopath, Inc., Charleston, SC, United States, [2] Department of Cell and Molecular Pharmacology & Experimental Therapeutics, Medical University of South Carolina, Charleston, SC, United States, [3] Department of Medicine, Gastroenterology and Hepatology, University of California San Diego, San Diego, CA, United States, [4] Digestive Disease Research Center, Medical University of South Carolina, Charleston, SC, United States

Our group has recently developed the GlycoTyper assay which is a streamlined antibody capture slide array approach to directly profile N-glycans of captured serum glycoproteins including immunoglobulin G (IgG). This method needs only a few microliters of serum and utilizes a simplified processing protocol that requires no purification or sugar modifications prior to analysis. In this method, antibody captured glycoproteins are treated with peptide N-glycosidase F (PNGase F) to release N-glycans for detection by MALDI imaging mass spectrometry (IMS). As alterations in N-linked glycans have been reported for IgG from large patient cohorts with fibrosis and cirrhosis, we utilized this novel method to examine the glycosylation of total IgG, as well as IgG1, IgG2, IgG3 and IgG4, which have never been examined before, in a cohort of 106 patients with biopsy confirmed liver fibrosis. Patients were classified as either having no evidence of fibrosis (41 patients with no liver disease or stage 0 fibrosis), early stage fibrosis (10 METAVIR stage 1 and 18 METAVIR stage 2) or late stage fibrosis (6 patients with METAVIR stage 3 fibrosis and 37 patients with METAVIR stage 4 fibrosis (cirrhosis)). Several major alterations in glycosylation were observed that classify patients as having no fibrosis (sensitivity of 92% and a specificity of 90%), early fibrosis (sensitivity of 84% with 90% specificity) or significant fibrosis (sensitivity of 94% with 90% specificity).

Keywords: glycosylation, immunoglobulin, fibrosis, cirrhosis, biomarker

## INTRODUCTION

Cirrhosis is the result of chronic liver injury and leads to replacement of the normal liver architecture by fibrotic scar tissue, and is associated with a concomitant decline of liver function and devastating clinical complications (1). Many different underlying processes cause cirrhosis: chronic viral infection by hepatitis B virus (HBV) and/or hepatitis C virus (HCV) have been

historically among the most common etiologies, but non-alcoholic fatty liver disease and ethanol are currently emerging as the leading causes of chronic liver disease worldwide.

For HBV and/or HCV infected patients, treatment decisions are based upon a variety of factors, including elevated levels of hepatic transaminases which may reflect the degree of hepatic inflammation and perhaps fibrosis when combined with other features such as platelet count (2, 3). Historically, in individuals with HBV or HCV, advanced fibrosis and cirrhosis are considered justifications to begin antiviral therapy (2, 4, 5). More importantly, the determination of hepatic fibrosis is critical to stage the severity of the liver disease and has been associated with prognosis (6). Therefore, it is extremely important to determine the presence of significant fibrosis and cirrhosis. Although liver biopsy has been historically the gold standard for assessment of fibrosis (7) noninvasive assessment of fibrosis is less intrusive and will allow for routine clinical monitoring.

Analysis of disease associated changes in total N-glycan compositions of serum and plasma in large patient cohorts has been previously reported (8, 9). There has also been extensive evaluation of disease-associated alterations of immunoglobin G N-linked glycans in large sample cohorts in patients with rheumatoid arthritis, digestive diseases, heart disease, cancer and liver fibrosis (10–34). In the case of liver fibrosis, two analytical methods have identified alterations in N-linked glycosylation on both total IgG populations and on specific IgG molecules. Both methods can detect cirrhosis with a high degree of accuracy and are also able to detect intermediate levels of fibrosis (11, 16). However, both analytical methods have drawbacks. One approach utilizes a capillary electrophoresis-based analysis of N-linked glycans on total serum following release of glycans using PNGase F, labeling of the released glycans using a fluorescent dye, and electrophoresis of the released glycans for peak identification (11). While this method works well, it is both time and labor intensive. Another method for liver fibrosis identification from serum utilizes a plate-based ELISA format to detect altered glycosylation using a sugar binding protein called a lectin (16). This test is hampered by the poor specificity of lectins and the limited readout (i.e. binding or not). Both of these methods require specialized sample handling resources, extensive processing and purification prior to analysis, and are expensive in regard to reagents and processing.

Our group has recently developed the GlycoTyper, a streamlined antibody capture slide array approach to directly profile N-glycans of captured serum glycoproteins like IgG. The method needs only a few microliters of serum and utilizes simplified processing workflows that requires no purification or sugar derivatizations as a part of the analysis. In this method, N-linked glycans are released from antibody captured glycoproteins and are directly analyzed by MALDI IMS, building on the utility of MALDI MS glycan imaging developed in our laboratories (35–48). Here, we have used the GlycoTyper to demonstrate its ability to measure changes in the N-linked glycans on IgG subtypes and serve as a surrogate marker of liver disease.

## MATERIALS AND METHODS

### Patients

Samples were from two main sources. The first was from the University of California at San Diego and the second from the Medical University of South Carolina. In both cases, the study protocol was approved by the appropriate Institutional Review Board and written informed consent was obtained from each subject. Demographic and clinical information was obtained, and a blood sample was collected from each subject. All liver biopsies were graded using the METAVIR scoring system (49). The etiology of the liver disease for the patients without viral infection was determined as previously described (50) and cirrhosis was determined based on histologic and/or clinical findings (i.e., clinical features of portal hypertension, with no alternative cause of portal hypertension). Details on all patients are provided in **Table 1**. A group of individuals with no history of liver disease, alcohol consumption less than 40 g a week, and no risk factors for viral hepatitis were utilized as controls. All subjects in this control group were documented to have normal liver biochemistry and negative HCV antibodies or HBV.

### Antibody Array Preparation

The serum assay used a 24-well slide module (Grace -Bio Labs, Bend, OR) that was mounted to a nitrocellulose-coated microscope slides (Grace-Bio Labs, Bend, OR). Antibodies: anti-human (IgG (Bethyl Labs, Montgomery, TX) anti-IgG1 (Abcam, Cambridge, UK), anti-IgG2, anti IgG-3, and anti-IgG 4 (Bio-Rad,

---

**TABLE 1** | Description of control patients and those with liver fibrosis.

| Variables | Controls | Stage of Fibrosis (METAVIR)[1] | | | | |
|---|---|---|---|---|---|---|
| | | 0 | 1 | 2 | 3 | 4 |
| Sample Size | 38 | 3 | 10 | 18 | 6 | 37 |
| Age[2] | 51 ± 11 | 56 ± 7 | 50 ± 6 | 51 ± 4 | 51 ± 7 | 55 ± 8 |
| % NHW/AA/H/Asian[3] | NA | 100/0/0/0 | 98/1/1/0 | 96/2/1/1 | 100/0/0/0 | 98/0/1/0 |
| ALT (IU/mL)[4] | NA | 75 ± 7 | 71 ± 11 | 78 ± 9 | 72 ± 12 | 85 ± 26 |
| AST (IU/mL)[5] | NA | 73 ± 5 | 69 ± 8 | 77 ± 10 | 78 ± 13 | 108 ± 24 |
| Total Bilirubin (mg/dL) | NA | 0.3 ± 0.2 | 0.3 ± 0.4 | 0.5 ± 0.4 | 0.9 ± 1.2 | 1.2 ± 1.3 |

[1]Fibrosis staging based upon METAVIR scoring system. [2]Mean age in years. [3]NHW, non-Hispanic White; AA, African American; H, Hispanic; [4]ALT, alanine aminotransferase; [5]AST, aspartate aminotransferase.
NA, not applicable.

Hercules, CA), were diluted in PBS and manually spotted in wells at 200 ng per 1.5 μL spot. Spots were then left to adhere overnight at 4°C in a humidity chamber made from cell culture dishes lined with a Wypall X 60 paper towel and two rolled KimWipes saturated with distilled water. Slides were then placed in a vacuum desiccator to dry at room temperature and rinsed for 1 minute with 200 μL 0.1% octyl-β-D- glucopyranoside in PBS (referred to as PBS-OGS) per well to remove any unbound protein from the slide. More detail on slide preparation and the general GlycoTyper method can be found in (41, 42).

## Sample Capture and N-Glycan Release

Antibody spots were blocked with 200 μL of 2% BSA (prepared in PBS-OGS) per well for 1 h with gentle shaking, washed with 200 μL PBS (3 min × 2) and 200 μL double distilled water (1 min × 1) per well and dried in a desiccator. Pure protein (0.5μg in 100 μL) or serum samples (diluted 1:100 in PBS to a total volume of 100 μL) were added to wells and incubated at room temperature for 2 hours in a humidity chamber with gentle shaking. Pure proteins: human IgG (Jackson ImmunoResearch Laboratories, West Grove, PA), human IgG1, IgG2, IgG3 and IgG4 (Abcam, Cambridge, UK). Wells were then serially washed with 200 μL of PBS-OGS (1 min ×2), 200μL PBS (3 min ×2), 200 μL double distilled water (1 min ×2), and dried. The well module was removed, and slides were dried in a vacuum desiccator. PNGase F Prime PRIME-LY (N-Zyme Scientifics, Doylestown, PA) (0.1 μg/μL in HPLC grade water) was applied to the slides using an automated sprayer (M5 TM-Sprayer, HTX Technologies, Chapel Hill, NC). Spatial localization to each capture spot was accomplished using spraying parameters of 15 passes at 45°C, 10 psi, flow rate of 25 μL/min, and 1200 mm/min velocity. Slides were incubated overnight at 37°C in humidity chambers made in cell culture dishes with Wypall X 60 paper towels and two rolled KimWipes saturated with distilled water.

## MALDI MS Preparation and Imaging

MALDI matrix α-cyano-4-hydroxycinnamic acid (CHCA, 7 mg/mL in 50% acetonitrile/0.1% trifluoroacetic acid) (Cayman Chemical, Ann Arbor, MI) was applied to slides using the same automated sprayer. Matrix was sprayed for two passes at 77°C, 10 psi, 1300 mm/min velocity, and flow rate of 100 μL/min. MALDI IMS data were acquired on a solariX Legacy 7T FT-ICR mass spectrometer (Bruker, Billerica, MA) equipped with a SmartBeam II laser operating at 2000 Hz and pixel dimension of 25 μm. Images were collected using a smartwalk pattern at a 300 μm raster with 200 laser shots per pixel. Samples were analyzed in positive ion with a mass range of 500–5000 m/z using a 512k word time domain. An on-slide resolving power of 58,000 at m/z 1501 was calculated.

## Data Analysis

N-Glycan localization and intensity were visualized using FlexImaging v5.0 (Bruker), with data imported at a 0.98 ICR reduction noise threshold. Images were normalized to total ion current, and N-glycan peaks were selected manually based on their theoretical mass values. For quantification of peaks at individual spots, spectra were imported into SCiLS Lab software 2017a (Bruker). Each spot was designated a unique region, and area under monoisotopic peak values were exported from each region and quantified by mean peak intensity. In all cases, glycan peaks (specific m/z values) were given a relative percentile of the total glycan profile. Glycan names are provided using the Oxford Nomenclature (51).

## Statistical Analysis

Patients were grouped as those: i) without any liver disease (healthy and stage 0), ii) with early to moderate fibrosis (stage 1 &2), and iii) with advanced fibrosis or cirrhosis (stage 3&4). One-way ANOVA and *Post hoc* tests were applied to inference any statistical difference among these three stages. Glycans with no statistical difference among stages (p>0.05, F-test) were discarded from further model development.
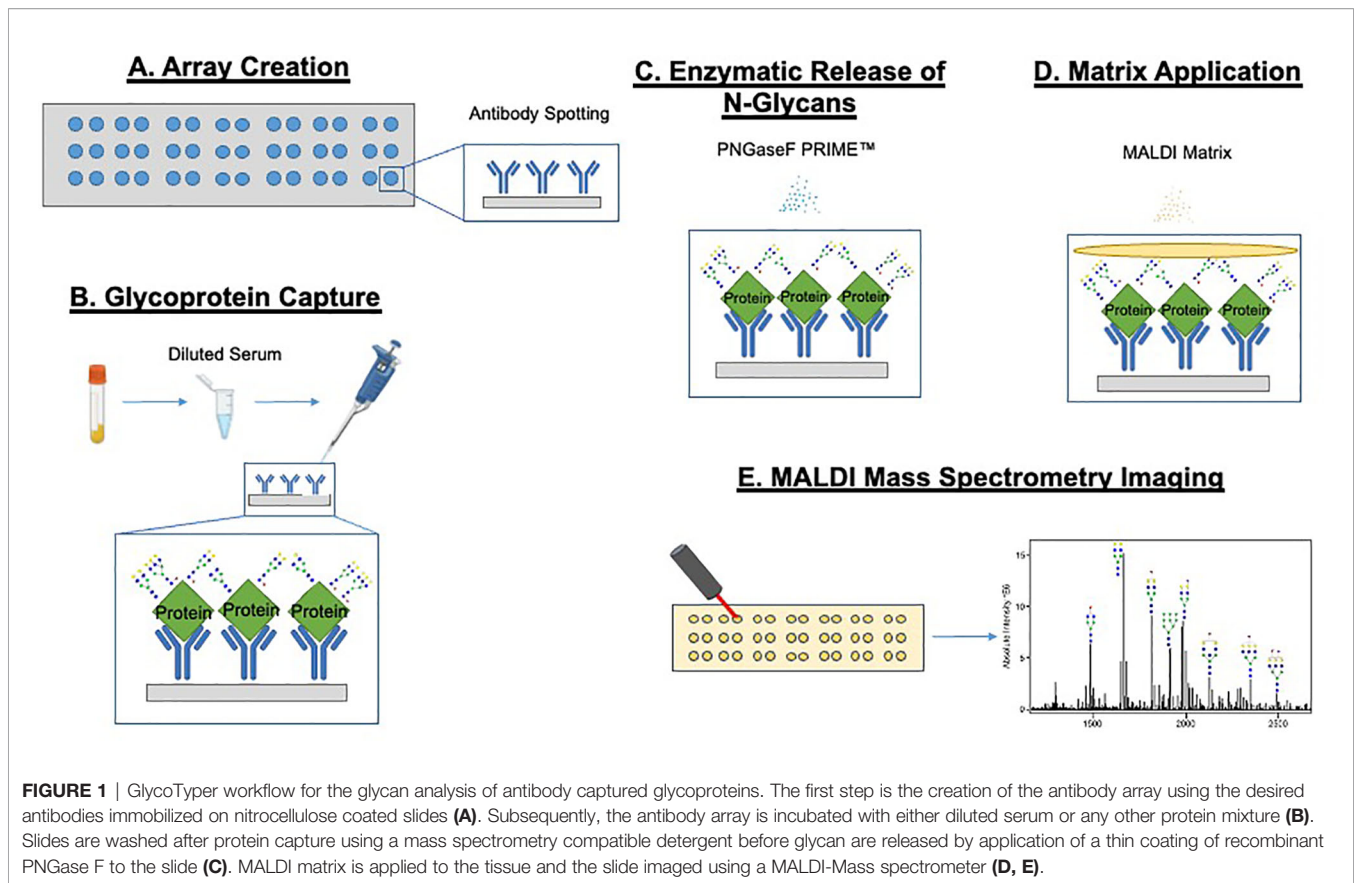
Subsequently, we applied the supervised learning algorithm random forest to determine the relative importance of the remaining features (glycans). Simultaneously, we applied variable clustering to perform a hierarchical cluster analysis, which is based on the similarity matrix that contains pairwise Hoeffding D statistics (52). From the variable clustering output, the most highly correlated two features were identified. These two features' relative importance were derived from random forest analysis. We discarded one of these pairs with lower importance. Then we utilized the remaining features in Apparent Cross-Validation, Leave-One-Out Cross-Validation, 3-Fold Random Subsampling Cross-Validation, and Repeated 3-Fold Cross-Validation to valuate predictive performance of the current random forest model (simulation 200 times for 3-Fold Random Subsampling Cross-Validation and Repeated 3-Fold Cross-Validation). Predictive accuracy (%), related sensitivity, specificity, positive predictive value (PPV), and negative predictive value (NPV) were criteria of model selection. The entire procedure (random forest, variable clustering; cross-validations) was iterated until the removal of any additional features resulted in the predictive ability of the model to consistently and dramatically deteriorated. The final model had the best predictive ability with the fewest features and was composed of glycans (features) from four of the IgG subtypes. These were A2G2F and A2BG0F on IgG, A2G1F and A2G2S1 on IgG1, A2G1F and A2G0F on IgG2 and A2BG1F on IgG3.

Finally, we evaluated our final model's discriminating ability between the following groups: no fibrosis vs moderate fibrosis, moderate vs later fibrosis, and no fibrosis vs later fibrosis. Four Cross-Validations listed above was applied and the corresponding AUCs (area under the curve), specificities, sensitivities, PPVs, and NPVs were derived.

More detail on feature selection, cross validation and model development can be found in the **Supplementary Evidence File**.

## RESULTS

The basic GlycoTyper workflow for the glycan analysis of antibody captured glycoproteins is shown in **Figure 1**. Briefly, the first step is the creation of the antibody array using the desired antibodies immobilized on nitrocellulose

**FIGURE 1** | GlycoTyper workflow for the glycan analysis of antibody captured glycoproteins. The first step is the creation of the antibody array using the desired antibodies immobilized on nitrocellulose coated slides **(A)**. Subsequently, the antibody array is incubated with either diluted serum or any other protein mixture **(B)**. Slides are washed after protein capture using a mass spectrometry compatible detergent before glycan are released by application of a thin coating of recombinant PNGase F to the slide **(C)**. MALDI matrix is applied to the tissue and the slide imaged using a MALDI-Mass spectrometer **(D, E)**.

coated slides (**Figure 1A**). Subsequently, the antibody array is incubated with either diluted serum or pure protein as shown in **Figure 1B**. Slides are washed after protein capture using a mass spectrometry compatible detergent before glycans are released by application of a thin coating of recombinant PNGase F PRIME™ to the slide (**Figure 1C**). This step is identical to what is performed in tissue glycan imaging (35, 42). Lastly, MALDI matrix is applied to the slide and is imaged using a MALDI Mass Spectrometer (**Figures 1D, E**). Importantly, the spatial localization provided by the IMS data link the detected glycans to their corresponding captured glycoproteins.

In initial studies, we examined the glycans on IgG, IgG1, IgG2, IgG3 and IgG4 captured *via* antibody from pure proteins spiked into PBS or from healthy serum diluted in PBS. As **Figure 2** shows for all proteins, the glycan observed from the pure protein was similar to that observed from captured human serum, with little difference in the glycosylation observed on the pure protein and that observed from the serum captured protein (with a single exception). The major exception was a glycan at m/z 1976.7822, which matches by accurate mass to a bi-antennary glycan with a single sialic acid (A2G2S1). In all cases, the level of this glycan was lower in the pure protein than that observed in human serum. In addition, a glycan at a glycan at m/z 1809.73273, which matches by accurate mass to a bi-antennary glycan with a single fucose residue was also varied in IgG2 and IgG3. **Supplementary Table S1** shows all the glycans found associated with IgG, IgG1, IgG2,

IgG3 or IgG4 and **Supplementary Figure S1** shows a column chart of the data in **Figure 1**.

The major glycan observed for each immunoglobulin subtype was a fucosylated biantennary glycan with single or double galactose residues, with or without a bisecting N-acetyl glucosamine (**Figure 2**). It is noted that the glycan profile observed from both samples was consistent with the glycan profile observed by other methods for these proteins (16, 53–59).

## Simultaneous Analysis of the Glycans on IgG, IgG1, IgG2, IgG3 and IgG4 in Patients With Liver Fibrosis

As previously reported, the glycosylation of IgG is altered with the development of liver fibrosis and cirrhosis and therefore can be used as a non-invasive measure of liver disease (11, 16, 18, 20, 30). Thus, the GlycoTyper method described in **Figure 1** was used for the analysis of a cohort of patients with biopsy confirmed fibrosis (**Table 1**). In total, 38 healthy individuals with no evidence of liver disease, 3 patients with stage 0 fibrosis (METAVIR), 10 patients with stage 1 fibrosis (METAVIR), 18 patients with stage 2 fibrosis (METAVIR), 6 patients with stage 3 fibrosis (METAVIR) and 37 patients with stage 4 fibrosis (METAVIR) were analyzed using this method. Because of the limited patient number, we grouped samples into three categories: i) those who are healthy with no fibrosis (healthy & METAVIR stage 0; n=41), ii) those with early to moderate fibrosis (METAVIR stages 1&2, n=28), and iii) those
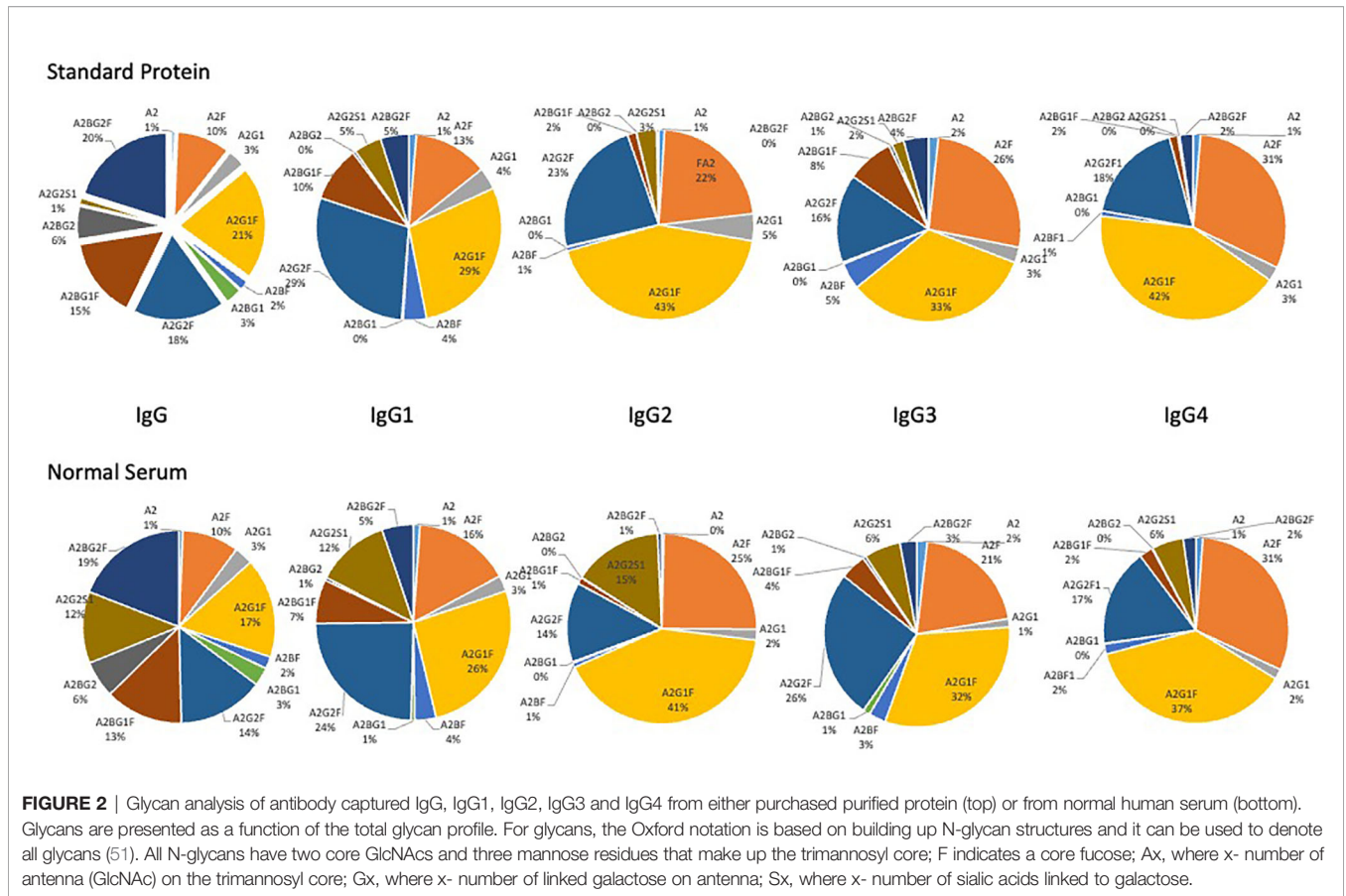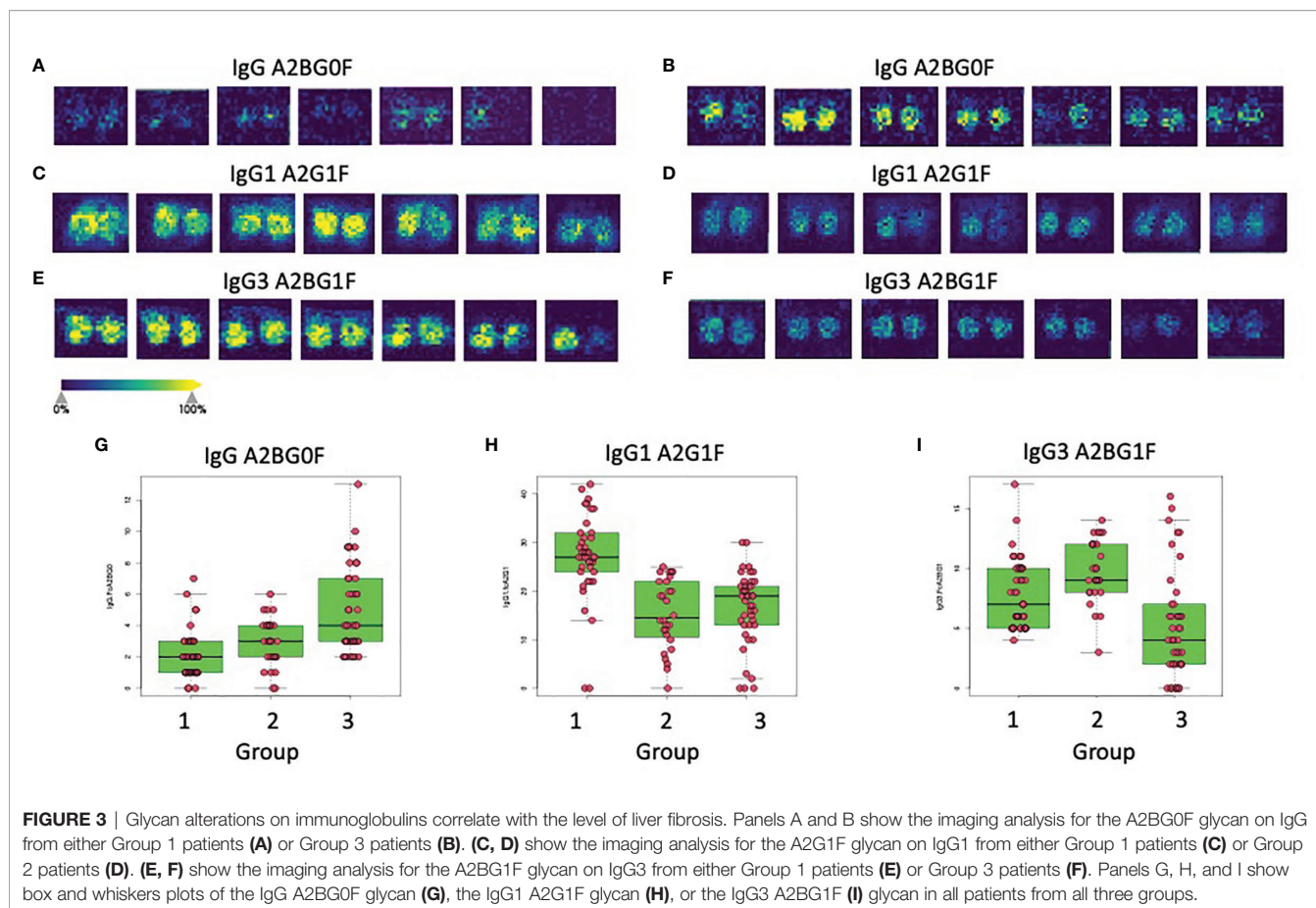
**FIGURE 2** | Glycan analysis of antibody captured IgG, IgG1, IgG2, IgG3 and IgG4 from either purchased purified protein (top) or from normal human serum (bottom). Glycans are presented as a function of the total glycan profile. For glycans, the Oxford notation is based on building up N-glycan structures and it can be used to denote all glycans (51). All N-glycans have two core GlcNAcs and three mannose residues that make up the trimannosyl core; F indicates a core fucose; Ax, where x- number of antenna (GlcNAc) on the trimannosyl core; Gx, where x- number of linked galactose on antenna; Sx, where x- number of sialic acids linked to galactose.

**TABLE 2** | Glycans that differentiate either early fibrosis from healthy, late fibrosis from early fibrosis or both.

| Early | Late | Early and Later |
|---|---|---|
| G4.A2G0F | G4.A2BG2F | G4.A2BG0F |
| G4.A2G1 | G.A2BG2F | G.A2G0F |
| G4.A2G1F | G1.A2G0F | G.A2BG0F |
| G4.A2G2F | G3.A2G2F | G.A2BG2F |
| G. A2BG0F | | G1.A2BG0F |
| G1.A2G2F | | G3.A2BG0F |
| G2.A2G0F | | |
| G2.A2G0F | | |
| G2.A2G1 | | |
| G2.A2G1F | | |
| G2.A2G2F | | |
| G2.A2BG1F | | |
| G2.A2BG2F | | |
| G3.A2G0F | | |
| G3.A2G1F | | |
| G3.A2G2F | | |

*For glycan names, the Oxford notation is used (51). All N-glycans have two core GlcNAcs and three mannose residues that make up the trimannosyl core; F indicates a core fucose; Ax, where x- number of antenna (GlcNAc) on the trimannosyl core; Gx, where x- number of linked galactose on antenna; Sx, where x- number of sialic acids linked to galactose. Using the G4.A2BG0F glycan as an example, G4 refers to IgG4, A2 indicates a bi-antennary glycan, the G0 indicates zero galactose residues, B represents the presence of a bisecting N-acetylglucosamine (GlcNAc), and the F indicated the presence of a fucose.*

with severe fibrosis and cirrhosis (METAVIR stage 3&4; n=43). **Table 2** lists those glycans that were statistically different (p<0.05) between the three patient groups. Glycans are classified as those that were altered in early-stage fibrosis only (as compared to healthy or stage 0 fibrosis) and do not alter further with fibrosis progression, glycans which alter only with the progression to significant fibrosis, and those glycans that are altered with both the development of early fibrosis and again with more significant fibrosis. **Figure 3** shows examples of three glycans that were altered on IgG, IgG1 and IgG3. One of the glycans with the greatest changes included a core fucosylated agalactosylated bi-antennary glycan with a bisecting N-acetyl glucosamine (A2BG0F, **Figures 3A, B**). As **Figure 3A** shows, this glycan was found at low levels in either healthy patients or patients with stage 0 fibrosis but increased dramatically in those with cirrhosis (**Figure 3B**). A2BG0F was found to increase in abundance in those patients with significant fibrosis/cirrhosis (Group 2), on both total IgG (**Figures 3A, B**) and to a lesser degree IgG1 and IgG3 (data not shown). In contrast, the A2G1F, a core fucosylated bi-antennary glycan with a single galactose residue found on IgG1, decreased in those patients with fibrosis (**Figures 3C, D**). Similarly, A2BG1F, a core fucosylated bi-antennary glycan with a single galactose residue and a bisecting N-acetyl glucosamine, found on IgG3 also decreased in those patients with fibrosis
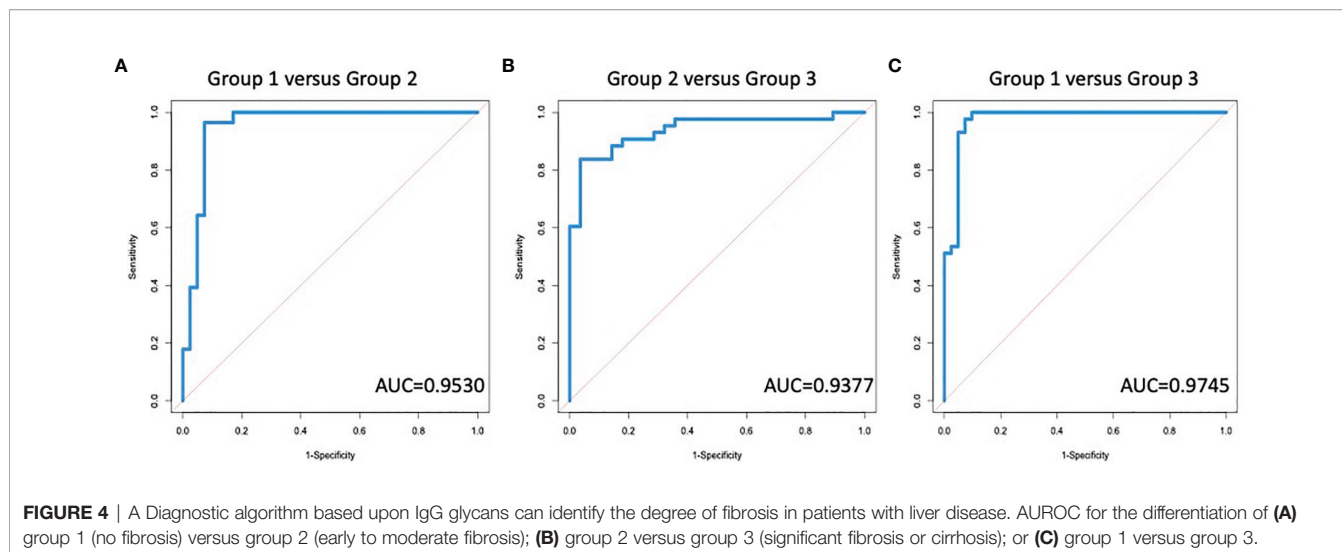
**FIGURE 3** | Glycan alterations on immunoglobulins correlate with the level of liver fibrosis. Panels A and B show the imaging analysis for the A2BG0F glycan on IgG from either Group 1 patients **(A)** or Group 3 patients **(B)**. **(C, D)** show the imaging analysis for the A2G1F glycan on IgG1 from either Group 1 patients **(C)** or Group 2 patients **(D)**. **(E, F)** show the imaging analysis for the A2BG1F glycan on IgG3 from either Group 1 patients **(E)** or Group 3 patients **(F)**. Panels G, H, and I show box and whiskers plots of the IgG A2BG0F glycan **(G)**, the IgG1 A2G1F glycan **(H)**, or the IgG3 A2BG1F **(I)** glycan in all patients from all three groups.

(**Figures 3E, F**). As **Figures 3E, F** demonstrate, this glycan was found at high levels in either healthy patients or patients with stage 0 fibrosis but was reduced dramatically in those with cirrhosis (**Figure 3F**).

The expression levels of both of these glycans also varied within the larger patient groups. In the case of IgG, the A2BG0F glycan increased from Group 1 to Group 2 and was the highest in Group 3, showing increased levels with increased fibrosis (**Figure 3G**). In contrast, IgG1 associated A2G1F glycan was reduced in patients with both limited and severe fibrosis and did not correlate with the state of fibrosis (**Figure 3H**). Other glycans such as the A2BG1F glycan on IgG3, was only reduced in patients with more significant fibrosis (Group 3, **Figure 3I**). A complete list of glycans that were altered in both those with mild to moderate fibrosis and those glycans altered with more significant fibrosis are shown in **Table 2**.

## Development of a Model to Determine the Level of Liver Fibrosis in Individuals Based Upon the IgG Glycan Profile

Based on our previous algorithm development work for the early detection of HCC (34, 60–62), we developed a random forest algorithm that could be used to differentiate individuals with early fibrosis (Group 2) from healthy controls (Group 1) as well as identify late fibrosis patients (Group 3) from those with early

fibrosis (Group 2). **Supplementary Table S2** shows the glycans that were found to be associated with IgG, IgG1, IgG2, IgG3 or IgG4 in all patient groups along with the results following ANOVA analysis. Although there were 50 glycans on the five subtypes of IgG that were altered with the development of liver fibrosis, many of these were associated and thus, only seven glycans on four glycoproteins were used to build and test the model. These are shown in **Supplementary Tables S3, S4** and include, A2G2F and A2BG0F on IgG, A2G1F and A2G2S1 on IgG1, A2G1F and A2G0F on IgG2 and A2BG1F on IgG3. **Figure 4A** shows the AUC (area under the curve) of the model following leave one out cross validation (LOOCV) when differentiating Group 1 (healthy and stage 0) from those with early or moderate fibrosis (Group 2; METAVIR stage 1 or 2). The AUC was 0.9530 (95%CI: 0.9008-1.0) for differentiating these two groups with a sensitivity of 94% at 90% specificity. Similar results were obtained using three-fold cross validation (3CV) (data not shown). When we compared those with early to moderate fibrosis (stage 1&2) to those with severe fibrosis or cirrhosis (stage 3 & 4), the AUC was 0.9377 (95%CI: 0.8819-0.9935) with a sensitivity of 84% at 90% specificity (**Figure 4B**). A further comparison was made to demonstrate that the AUC for differentiating those with no liver disease from those with significant fibrosis/cirrhosis (**Figure 4C**) and in this case, the AUC was 0.9745 (95%CI: 0.9415-1) with 98% sensitivity at 90% specificity. The

**FIGURE 4** | A Diagnostic algorithm based upon IgG glycans can identify the degree of fibrosis in patients with liver disease. AUROC for the differentiation of **(A)** group 1 (no fibrosis) versus group 2 (early to moderate fibrosis); **(B)** group 2 versus group 3 (significant fibrosis or cirrhosis); or **(C)** group 1 versus group 3.

sensitivity, specificity, positive and negative predictive values of the assay for differentiating the different groups are shown in **Supplementary Tables S5–S7**. In addition, a comparison between our assay and other noninvasive assays for the detection of liver fibrosis is shown in **Supplementary Table S8**. It is noted that in **Supplementary Table S8** the assay performance for the detection of ≥2 fibrosis or ≥4 fibrosis is compared, as these are the data most often presented for other markers.

We also examined the ability of these glycans (**Supplementary Figure S1**) to differentiate different groups of patients, specifically, those with no or early fibrosis (healthy and stage 0&1) from those with moderate to significant fibrosis (stage 2&3) and those with cirrhosis (stage 4) from those with moderate to significant fibrosis (stage 2&3). The AUC was 0.8464 (95%CI: 0.7576- 0.9352) for differentiating those with no or early fibrosis (healthy versus stage 0&1) from those with moderate to significant fibrosis (stage 2&3) but 0.9673 (95%CI: 0.93-1.0) when differentiating cirrhosis from moderate to significant fibrosis. These findings highlight that changes in IgG glycosylation can be observed *via* the GlycoTyper method and used to determine the level of liver fibrosis in individuals with liver disease.

## DISCUSSION

The GlycoTyper is an imaging mass spectrometry platform for the multiplexed detection of N-glycans from individual glycoproteins. This method is suitable for the analysis of immunoglobulin molecules from a wide variety of biological samples. The development of this technique was based on a well-established protocol for enzymatic release of N-glycans from tissue sections for MALDI IMS (63). In this platform, antibodies are essential for the specific capture of glycoprotein targets from a complex biological mixture, similar to an ELISA. However, unlike an ELISA, no secondary antibody or lectin is needed for this methodology as mass spectrometry provides sensitive and molecular specific detection of distinct N-glycans. Antibody capture also negates the

need for sample cleanup prior to MS analysis, which can be extensive (64).

We applied the GlycoTyper platform to the analysis of IgG glycans from patients with liver disease. As stated, changes in the glycosylation of immunoglobulins have been associated with liver fibrosis and cirrhosis previously and in many cases, those changes were detected with lectins or other indirect or laborious methods (16, 56). The results presented here show that these changes can be observed *via* the GlycoTyper method and furthermore, that these can be used to determine the level of liver fibrosis in individuals with liver disease. One of the major changes observed was an increase in the level of IgG associated glycans devoid of terminal galactose residues (**Figure 3**). This is a change that has been observed before and exploited with lectins (16). However, this was only one of numerous subtype specific glycan changes that were observed (**Figure 3**). These subtype specific glycan changes were used to create a diagnostic algorithm that could classify the level of fibrosis in individuals with high accuracy and specificity. It is noted that other glycoproteins have altered glycans in liver fibrosis and the methods described here could easily be applied to the analysis of those glycoproteins as well (65–69).

Our study was limited in part by the relatively small number of patients with histologically proven early stage liver disease (**Table 1**). This required clustering multiple patient groups together for further analysis. Consequently, patients were grouped into those with no fibrosis (Group 1), those with early to moderate fibrosis (Group 2) or late-stage fibrosis or cirrhosis (Group 3). We also attempted to classify patients into those with no to early fibrosis (healthy, stage 0&1), moderate to severe fibrosis (stage 2&3) and cirrhosis (stage 4). However, as shown in **Supplementary Figure S2**, diagnostic performance was poor in differentiating those with zero to early fibrosis from those with moderate to severe fibrosis. This was primarily the result of the stage 1 patients having an immunoglobulin glycan profile that was more similar to stage 2 patients than to stage 0 or healthy patients. This is an important point and clearly indicates that the

changes in glycosylation observed on immunoglobulins occurs early in fibrosis development. It is also noted that excellent discriminatory ability was observed between those with moderate to severe fibrosis and cirrhosis. However, this is most likely driven by the small number of patients with severe fibrosis (n=6) and the large glycan difference observed in patients with cirrhosis and moderate fibrosis. Larger, more diverse studies that include patients with different types of clinical liver diseases and a direct comparison to other non-invasive tests for cirrhosis required (3, 11, 70–73)

In conclusion, this study establishes a clinical rationale for integrating direct analysis of IgG glycans for the active management of people with liver disease. The diagnostic performance of this method was dramatically greater than other non-invasive tests for liver fibrosis (**Supplementary Table S8**), such as FIB4, APRI and even tests that look at IgG glycans (11, 16, 74). One reason for this is the ability to not just look at total IgG but also the specific IgG sub-classes, which has not been performed before, as such studies were not technically feasible for large patient cohorts. Thus, the methods described here are not only useful as a research tool for the analysis of protein specific glycosylation but also represents a new diagnostic platform that will allow for the true diagnostic potential of N-linked glycans to be developed.

## DATA AVAILABILITY STATEMENT

The original contributions presented in the study are included in the article/**Supplementary Material**. Further inquiries can be directed to the corresponding author.

## ETHICS STATEMENT

The studies involving human participants was reviewed and approved by the University of South California at San Diego and Medical University of South Carolina Review Board. The patients/participants provided their written informed consent to participate in research studies.

## REFERENCES

## SUPPLEMENTARY MATERIAL

The Supplementary Material for this article can be found online at: https://www.frontiersin.org/articles/10.3389/fimmu.2022.797460/full#supplementary-material

1. Rockey DC, Bell PD, Hill JA. Fibrosis–a Common Pathway to Organ Injury and Failure. *N Engl J Med* (2015) 372:1138–49. doi: 10.1056/NEJMra1300575
2. Fung SK, Lok AS. Management of Hepatitis B Patients With Antiviral Resistance. *Antivir Ther* (2004) 9:1013–26.
3. Sterling RK, Lissen E, Clumeck N, Sola R, Correa MC, Montaner J, et al. Development of a Simple Noninvasive Index to Predict Significant Fibrosis in Patients With HIV/HCV Coinfection. *Hepatology* (2006) 43:1317–25. doi: 10.1002/hep.21178
4. Kweon YO, Goodman ZD, Dienstag JL, Schiff ER, Brown NA, Burchardt E, et al. Decreasing Fibrogenesis: An Immunohistochemical Study of Paired Liver Biopsies Following Lamivudine Therapy for Chronic Hepatitis B. *J Hepatol* (2001) 35:749–55. doi: 10.1016/S0168-8278(01)00218-5
5. Sherman M. Hepatocellular Carcinoma: Epidemiology, Risk Factors, and Screening. *Semin Liver Dis* (2005) 25:143–54. doi: 10.1055/s-2005-871194
6. Liaw YF. Results of Lamivudine Trials in Asia. *J Hepatol* (2003) 39(Suppl 1): S111–5. doi: 10.1016/S0168-8278(03)00155-7
7. Rockey DC, Caldwell SH, Goodman ZD, Nelson RC, Smith ADAmerican Association for the Study of Liver, D. Liver Biopsy. *Hepatology* (2009) 49:1017–44. doi: 10.1002/hep.22742
8. Mehta A, Block TM. Fucosylated Glycoproteins as Markers of Liver Disease. *Dis Markers* (2008) 25:259–65. doi: 10.1155/2008/264594
9. Gudelj I, Lauc G, Pezer M. Immunoglobulin G Glycosylation in Aging and Diseases. *Cell Immunol* (2018) 333:65–79. doi: 10.1016/j.cellimm.2018.07.009
10. Callewaert N, Schollen E, Vanhecke A, Jaeken J, Matthijs G, Contreras R. Increased Fucosylation and Reduced Branching of Serum Glycoprotein N-Glycans in All Known Subtypes of Congenital Disorder of Glycosylation I. *Glycobiology* (2003) 13:367–75. doi: 10.1093/glycob/cwg040
11. Callewaert N, Van Vlierberghe H, Van Hecke A, Laroy W, Delanghe J, Contreras R. Noninvasive Diagnosis of Liver Cirrhosis Using DNA Sequencer Based Total Serum Protein Glycomics. *Nat Med* (2004) 10:429–34. doi: 10.1038/nm1006
12. Block TM, Comunale MA, Lowman M, Steel LF, Romano PR, Fimmel C, et al. Use of Targeted Glycoproteomics to Identify Serum Glycoproteins That Correlate With Liver Cancer in Woodchucks and Humans. *Proc Natl Acad Sci USA* (2005) 102:779–84. doi: 10.1073/pnas.0408928102

13. Marrero JA, Romano PR, Nikolaeva O, Steel L, Mehta A, Fimmel CJ, et al. GP73, a Resident Golgi Glycoprotein, Is a Novel Serum Marker for Hepatocellular Carcinoma. *J Hepatol* (2005) 43:1007–12. doi: 10.1016/j.jhep.2005.05.028

14. Comunale MA, Lowman M, Long RE, Krakover J, Philip R, Seeholzer S, et al. Proteomic Analysis of Serum Associated Fucosylated Glycoproteins in the Development of Primary Hepatocellular Carcinoma. *J Proteome Res* (2006) 5:308–15. doi: 10.1021/pr050328x

15. Liu XE, Desmyter L, Gao CF, Laroy W, Dewaele S, Vanhooren V, et al. N-Glycomic Changes in Hepatocellular Carcinoma Patients With Liver Cirrhosis Induced by Hepatitis B Virus. *Zhonghua gan zang Bing Za Zhi = Zhonghua Ganzangbing Zazhi = Chin J Hepatol* (2008) 16:74–5. doi: 10.1002/hep.21855

16. Mehta AS, Long RE, Comunale MA, Wang M, Rodemich L, Krakover J, et al. Increased Levels of Galactose-Deficient Anti-Gal Immunoglobulin G in the Sera of Hepatitis C Virus-Infected Individuals With Fibrosis and Cirrhosis. *J Virol* (2008) 82:1259–70. doi: 10.1128/JVI.01600-07

17. Norton PA, Comunale MA, Krakover J, Rodemich L, Pirog N, D'amelio A, et al. N-Linked Glycosylation of the Liver Cancer Biomarker GP73. *J Cell Biochem* (2008) 104:136–49. doi: 10.1002/jcb.21610

18. Blomme B, Van Steenkiste C, Callewaert N, Van Vlierberghe H. Alteration of Protein Glycosylation in Liver Diseases. *J Hepatol* (2009) 50:592–603. doi: 10.1016/j.jhep.2008.12.010

19. Comunale MA, Wang M, Hafner J, Krakover J, Rodemich L, Kopenhaver B, et al. Identification and Development of Fucosylated Glycoproteins as Biomarkers of Primary Hepatocellular Carcinoma. *J Proteome Res* (2009) 8:595–602. doi: 10.1021/pr800752c

20. Vanderschaeghe D, Laroy W, Sablon E, Halfon P, Van Hecke A, Delanghe J, et al. Glycofibrotest Is a Highly Performant Liver Fibrosis Biomarker Derived From DNA Sequencer-Based Serum Protein Glycomics. *Mol Cell Proteomics: MCP* (2009) 8:986–94. doi: 10.1074/mcp.M800470-MCP200

21. Wang M, Long RE, Comunale MA, Junaidi O, Marrero J, Di Bisceglie AM, et al. Novel Fucosylated Biomarkers for the Early Detection of Hepatocellular Carcinoma: A Publication of the American Association for Cancer Research, Cosponsored by the American Society of Preventive Oncology. *Cancer Epidemiol Biomarkers Prev* (2009) 18:1914–21. doi: 10.1158/1055-9965.EPI-08-0980

22. Comunale MA, Rodemich-Betesh L, Hafner J, Wang M, Norton P, Di Bisceglie AM, et al. Linkage Specific Fucosylation of Alpha-1-Antitrypsin in Liver Cirrhosis and Cancer Patients: Implications for a Biomarker of Hepatocellular Carcinoma. *PloS One* (2010) 5:e12419. doi: 10.1371/journal.pone.0012419

23. Debruyne EN, Vanderschaeghe D, Van Vlierberghe H, Vanhecke A, Callewaert N, Delanghe JR. Diagnostic Value of the Hemopexin N-Glycan Profile in Hepatocellular Carcinoma Patients. *Clin Chem* (2010) 56:823–31. doi: 10.1373/clinchem.2009.139295

24. Vanderschaeghe D, Szekrenyes A, Wenz C, Gassmann M, Naik N, Bynum M, et al. High-Throughput Profiling of the Serum N-Glycome on Capillary Electrophoresis Microfluidics Systems: Toward Clinical Implementation of Glycohepatotest. *Anal Chem* (2010) 82:7408–15. doi: 10.1021/ac101560a

25. Blomme B, Van Steenkiste C, Grassi P, Haslam SM, Dell A, Callewaert N, et al. Alterations of Serum Protein N-Glycosylation in Two Mouse Models of Chronic Liver Disease Are Hepatocyte and Not B Cell Driven. *Am J Physiol Gastrointest Liver Physiol* (2011) 300:G833–42. doi: 10.1152/ajpgi.00228.2010

26. Comunale MA, Wang M, Rodemich-Betesh L, Hafner J, Lamontagne A, Klein A, et al. Novel Changes in Glycosylation of Serum Apo-J in Patients With Hepatocellular Carcinoma. *Cancer Epidemiol Biomarkers Prev* (2011) 20:1222–9. doi: 10.1158/1055-9965.EPI-10-1047

27. Blomme B, Francque S, Trepo E, Libbrecht L, Vanderschaeghe D, Verrijken A, et al. N-Glycan Based Biomarker Distinguishing Non-Alcoholic Steatohepatitis From Steatosis Independently of Fibrosis. *Dig Liver Dis* (2012) 44:315–22. doi: 10.1016/j.dld.2011.10.015

28. Mehta A, Norton P, Liang H, Comunale MA, Wang M, Rodemich-Betesh L, et al. Increased Levels of Tetra-Antennary N-Linked Glycan But Not Core Fucosylation Are Associated With Hepatocellular Carcinoma Tissue. *Cancer Epidemiol Biomarkers Prev* (2012) 21:925–33. doi: 10.1158/1055-9965.EPI-11-1183

29. Comunale MA, Wang M, Anbarasan N, Betesh L, Karabudak A, Moritz E, et al. Total Serum Glycan Analysis Is Superior to Lectin-FLISA for the Early Detection of Hepatocellular Carcinoma. *Proteomics Clin Appl* (2013) 7:690–700. doi: 10.1002/prca.201200125

30. Lamontagne A, Long RE, Comunale MA, Hafner J, Rodemich-Betesh L, Wang M, et al. Altered Functionality of Anti-Bacterial Antibodies in Patients With Chronic Hepatitis C Virus Infection. *PloS One* (2013) 8:e64992. doi: 10.1371/journal.pone.0064992

31. Vanderschaeghe D, Debruyne E, Van Vlierberghe H, Callewaert N, Delanghe J. CE Analysis of Gamma-Globulin Mobility and Potential Clinical Utility. *Methods Mol Biol* (2013) 919:249–57. doi: 10.1007/978-1-62703-029-8_22

32. Betesh L, Comunale MA, Wang M, Liang H, Hafner J, Karabudak A, et al. Identification of Fucosylated Fetuin-a as a Potential Biomarker for Cholangiocarcinoma. *Proteomics Clin Appl* (2017) 11:9–10. doi: 10.1002/prca.201600141

33. Verhelst X, Vanderschaeghe D, Castera L, Raes T, Geerts A, Francoz C, et al. A Glycomics-Based Test Predicts the Development of Hepatocellular Carcinoma in Cirrhosis. *Clin Cancer Res* (2017) 23:2750–8. doi: 10.1158/1078-0432.CCR-16-1500

34. Wang M, Sanda M, Comunale MA, Herrera H, Swindell C, Kono Y, et al. Changes in the Glycosylation of Kininogen and the Development of a Kininogen-Based Algorithm for the Early Detection of HCC. *Cancer Epidemiol Biomarkers Prev* (2017) 26:795–803. doi: 10.1158/1055-9965.EPI-16-0974

35. Powers TW, Neely BA, Shao Y, Tang H, Troyer DA, Mehta AS, et al. MALDI Imaging Mass Spectrometry Profiling of N-Glycans in Formalin-Fixed Paraffin Embedded Clinical Tissue Blocks and Tissue Microarrays. *PloS One* (2014) 9:e106255. doi: 10.1371/journal.pone.0106255

36. Powers TW, Holst S, Wuhrer M, Mehta AS, Drake RR. Two-Dimensional N-Glycan Distribution Mapping of Hepatocellular Carcinoma Tissues by MALDI-Imaging Mass Spectrometry. *Biomolecules* (2015) 5:2554–72. doi: 10.3390/biom5042554

37. Drake RR, Powers TW, Jones EE, Bruner E, Mehta AS, Angel PM. MALDI Mass Spectrometry Imaging of N-Linked Glycans in Cancer Tissues. *Adv Cancer Res* (2017) 134:85–116. doi: 10.1016/bs.acr.2016.11.009

38. Drake RR, Powers TW, Norris-Caneda K, Mehta AS, Angel PM. *In Situ* Imaging of N-Glycans by MALDI Imaging Mass Spectrometry of Fresh or Formalin-Fixed Paraffin-Embedded Tissue. *Curr Protoc Protein Sci* (2018) 94:e68. doi: 10.1002/cpps.68

39. Drake RR, West CA, Mehta AS, Angel PM. MALDI Mass Spectrometry Imaging of N-Linked Glycans in Tissues. *Adv Exp Med Biol* (2018) 1104:59–76. doi: 10.1007/978-981-13-2158-0_4

40. West CA, Wang M, Herrera H, Liang H, Black A, Angel PM, et al. N-Linked Glycan Branching and Fucosylation Are Increased Directly in Hcc Tissue as Determined Through in Situ Glycan Imaging. *J Proteome Res* (2018) 17:3454–62. doi: 10.1021/acs.jproteome.8b00323

41. Black AP, Angel PM, Drake RR, Mehta AS. Antibody Panel Based N-Glycan Imaging for N-Glycoprotein Biomarker Discovery. *Curr Protoc Protein Sci* (2019) 98:e99. doi: 10.1002/cpps.99

42. Black AP, Liang H, West CA, Wang M, Herrera HP, Haab BB, et al. A Novel Mass Spectrometry Platform for Multiplexed N-Glycoprotein Biomarker Discovery From Patient Biofluids by Antibody Panel Based N-Glycan Imaging. *Anal Chem* (2019) 91:8429–35. doi: 10.1021/acs.analchem.9b01445

43. Scott DA, Casadonte R, Cardinali B, Spruill L, Mehta AS, Carli F, et al. Increases in Tumor N-Glycan Polylactosamines Associated With Advanced HER2-Positive and Triple-Negative Breast Cancer Tissues. *Proteomics Clin Appl* (2019) 13:e1800014. doi: 10.1002/prca.201800014

44. Scott DA, Norris-Caneda K, Spruill L, Bruner E, Kono Y, Angel PM, et al. Specific N-Linked Glycosylation Patterns in Areas of Necrosis in Tumor Tissues. *Int J Mass Spectrom* (2019) 437:69–76. doi: 10.1016/j.ijms.2018.01.002

45. Blaschke CRK, Black AP, Mehta AS, Angel PM, Drake RR. Rapid N-Glycan Profiling of Serum and Plasma by a Novel Slide-Based Imaging Mass Spectrometry Workflow. *J Am Soc Mass Spectrom* (2020) 12:2511–20. doi: 10.1021/jasms.0c00213

46. Drake RR, Mcdowell C, West C, David F, Powers TW, Nowling T, et al. Defining the Human Kidney N-Glycome in Normal and Cancer Tissues Using MALDI Imaging Mass Spectrometry. *J Mass Spectrom* (2020) 55:e4490. doi: 10.1002/jms.4490

47. West CA, Liang H, Drake RR, Mehta AS. New Enzymatic Approach to Distinguish Fucosylation Isomers of N-Linked Glycans in Tissues Using MALDI Imaging Mass Spectrometry. *J Proteome Res* (2020) 19(8):2989–96. doi: 10.1021/acs.jproteome.0c00024

48. Delacourt A, Black A, Angel P, Drake R, Hoshida Y, Singal A, et al. N-Glycosylation Patterns Correlate With Hepatocellular Carcinoma Genetic Subtypes. *Mol Cancer Res* (2021) 19(11):1686–77. doi: 10.1158/1541-7786.MCR-21-0348

49. Goodman ZD. Grading and Staging Systems for Inflammation and Fibrosis in Chronic Liver Diseases. *J Hepatol* (2007) 47:598–607. doi: 10.1016/j.jhep.2007.07.006

50. Marrero JA, Fontana RJ, Su GL, Conjeevaram HS, Emick DM, Lok AS. NAFLD may be a Common Underlying Liver Disease in Patients With Hepatocellular Carcinoma in the United States. *Hepatology* (2002) 36:1349–54. doi: 10.1002/hep.1840360609

51. Harvey DJ, Merry AH, Royle L, Campbell MP, Dwek RA, Rudd PM. Proposal for a Standard System for Drawing Structural Diagrams of N- and O-Linked Carbohydrates and Related Compounds. *Proteomics* (2009) 9:3796–801. doi: 10.1002/pmic.200900096

52. Hoeffding W. A Non-Parametric Test of Independence. *Ann Math Stat* (1948) 19:546–57. doi: 10.1214/aoms/1177730150

53. Malhotra R, Wormald MR, Rudd PM, Fischer PB, Dwek RA, Sim RB. Glycosylation Changes of Igg Associated With Rheumatoid Arthritis can Activate Complement via the Mannose-Binding Protein. *Nat Med* (1995) 1:237–43. doi: 10.1038/nm0395-237

54. Wormald MR, Rudd PM, Harvey DJ, Chang SC, Scragg IG, Dwek RA. Variations in Oligosaccharide-Protein Interactions in Immunoglobulin G Determine the Site-Specific Glycosylation Profiles and Modulate the Dynamic Motion of the Fc Oligosaccharides. *Biochemistry* (1997) 36:1370–80. doi: 10.1021/bi9621472

55. Saphire EO, Stanfield RL, Crispin MD, Morris G, Zwick MB, Pantophlet RA, et al. Crystal Structure of an Intact Human IgG: Antibody Asymmetry, Flexibility, and a Guide for HIV-1 Vaccine Design. *Adv Exp Med Biol* (2003) 535:55–66. doi: 10.1007/978-1-4615-0065-0_4

56. Saldova R, Royle L, Radcliffe CM, Abd Hamid UM, Evans R, Arnold JN, et al. Ovarian Cancer Is Associated With Changes in Glycosylation in Both Acute-Phase Proteins and IGG. *Glycobiology* (2007) 17:1344–56. doi: 10.1093/glycob/cwm100

57. Bones J, Mittermayr S, O'donoghue N, Guttman A, Rudd PM. Ultra Performance Liquid Chromatographic Profiling of Serum N-Glycans for Fast and Efficient Identification of Cancer Associated Alterations in Glycosylation. *Anal Chem* (2010) 82:10208–15. doi: 10.1021/ac102860w

58. Pucic M, Knezevic A, Vidic J, Adamczyk B, Novokmet M, Polasek O, et al. High Throughput Isolation and Glycosylation Analysis of Igg-Variability and Heritability of the IGG Glycome in Three Isolated Human Populations. *Mol Cell Proteomics* (2011) 10:M111 010090. doi: 10.1074/mcp.M111.010090

59. Coss KP, Byrne JC, Coman DJ, Adamczyk B, Abrahams JL, Saldova R, et al. Igg N-Glycans as Potential Biomarkers for Determining Galactose Tolerance in Classical Galactosaemia. *Mol Genet Metab* (2012) 105:212–20. doi: 10.1016/j.ymgme.2011.10.018

60. Wang M, Block TM, Marrero J, Di Bisceglie AM, Devarajan K, Mehta A. (2012). Improved Biomarker Performance for the Detection of Hepatocellular Carcinoma by Inclusion of Clinical Parameters. *Proc IEEE Int Conf Bioinformatics Biomed* (2012) 10.1109/BIBM.2012.6392612. doi: 10.1109/BIBM.2012.6392612

61. Wang M, Mehta A, Block TM, Marrero J, Di Bisceglie AM, Devarajan K. A Comparison of Statistical Methods for the Detection of Hepatocellular Carcinoma Based on Serum Biomarkers and Clinical Variables. *BMC Med Genomics* (2013) 6:S9. doi: 10.1186/1755-8794-6-S3-S9

62. Wang M, Devarajan K, Singal AG, Marrero JA, Dai J, Feng Z, et al. The Doylestown Algorithm: A Test to Improve the Performance of AFP in the Detection of Hepatocellular Carcinoma. *Cancer Prev Res (Phila)* (2016) 9:172–9. doi: 10.1158/1940-6207.CAPR-15-0186

63. Powers TW, Jones EE, Betesh LR, Romano PR, Gao P, Copland JA, et al. Matrix Assisted Laser Desorption Ionization Imaging Mass Spectrometry Workflow for Spatial Profiling Analysis of N-Linked Glycan Expression in Tissues. *Anal Chem* (2013) 85:9799–806. doi: 10.1021/ac402108x

64. Ruhaak LR, Huhn C, Waterreus WJ, De Boer AR, Neususs C, Hokke CH, et al. Hydrophilic Interaction Chromatography-Based High-Throughput Sample Preparation Method for N-Glycan Analysis From Total Human Plasma Glycoproteins. *Anal Chem* (2008) 80:6119–26. doi: 10.1021/ac800630x

65. Shirabe K, Bekki Y, Gantumur D, Araki K, Ishii N, Kuno A, et al. Mac-2 Binding Protein Glycan Isomer (M2bpgi) Is a New Serum Biomarker for Assessing Liver Fibrosis: More Than a Biomarker of Liver Fibrosis. *J Gastroenterol* (2018) 53:819–26. doi: 10.1007/s00535-017-1425-z

66. Cao X, Shang QH, Chi XL, Zhang W, Xiao HM, Sun MM, et al. Serum N-Glycan Markers for Diagnosing Liver Fibrosis Induced by Hepatitis B Virus. *World J Gastroenterol* (2020) 26:1067–79. doi: 10.3748/wjg.v26.i10.1067

67. Higashi M, Yoshimura T, Usui N, Kano Y, Deguchi A, Tanabe K, et al. A Potential Serum N-Glycan Biomarker for Hepatitis C Virus-Related Early-Stage Hepatocellular Carcinoma With Liver Cirrhosis. *Int J Mol Sci* (2020) 21:8913–25. doi: 10.3390/ijms21238913

68. Ogawa K, Kobayashi T, Furukawa JI, Hanamatsu H, Nakamura A, Suzuki K, et al. Tri-Antennary Tri-Sialylated Mono-Fucosylated Glycan of Alpha-1 Antitrypsin as a Non-Invasive Biomarker for Non-Alcoholic Steatohepatitis: A Novel Glycobiomarker for Non-Alcoholic Steatohepatitis. *Sci Rep* (2020) 10:321. doi: 10.1038/s41598-019-56947-1

69. Verhelst X, Dias AM, Colombel JF, Vermeire S, Van Vlierberghe H, Callewaert N, et al. Protein Glycosylation as a Diagnostic and Prognostic Marker of Chronic Inflammatory Gastrointestinal and Liver Diseases. *Gastroenterology* (2020) 158:95–110. doi: 10.1053/j.gastro.2019.08.060

70. Myers RP, Ratziu V, Imbert-Bismut F, Charlotte F, Poynard T. Biochemical Markers of Liver Fibrosis: A Comparison With Historical Features in Patients With Chronic Hepatitis C. *Am J Gastroenterol* (2002) 97:2419–25. doi: 10.1111/j.1572-0241.2002.05997.x

71. Myers RP, Benhamou Y, Imbert-Bismut F, Thibault V, Bochet M, Charlotte F, et al. Serum Biochemical Markers Accurately Predict Liver Fibrosis in HIV and Hepatitis C Virus Co-Infected Patients. *Aids* (2003) 17:721–5. doi: 10.1097/00002030-200303280-00010

72. Myers RP, De Torres M, Imbert-Bismut F, Ratziu V, Charlotte F, Poynard T. Biochemical Markers of Fibrosis in Patients With Chronic Hepatitis C: A Comparison With Prothrombin Time, Platelet Count, and Age-Platelet Index. *Dig Dis Sci* (2003) 48:146–53. doi: 10.1023/A:1021702902681

73. Rossi E, Adams L, Prins A, Bulsara M, De Boer B, Garas G, et al. Validation of the Fibrotest Biochemical Markers Score in Assessing Liver Fibrosis in Hepatitis C Patients. *Clin Chem* (2003) 49:450–4. doi: 10.1373/49.3.450

74. Younes R, Caviglia GP, Govaere O, Rosso C, Armandi A, Sanavia T, et al. Long-Term Outcomes and Predictive Ability of Non-Invasive Scoring Systems in Patients With Non-Alcoholic Fatty Liver Disease. *J Hepatol* (2021) 75:786–94. doi: 10.1016/j.jhep.2021.05.008